

# Measurement of the sensitivity of heterodyne detection to aberrations using a programmable liquid-crystal modulator

Dominique Delautre <sup>a,\*</sup>, Sébastien Breugnot <sup>a</sup>, Vincent Laude <sup>b</sup>

<sup>a</sup> Thomson-CSF Optronique, Rue Guynemer, BP 55, 78283 Guyancourt, France

<sup>b</sup> Thomson-CSF, Corporate Research Laboratories, Domaine de Corbeville, 91404 Orsay Cedex, France

Received 9 October 1998; revised 24 November 1998; accepted 25 November 1998

---

## Abstract

Heterodyne detection is known to be highly sensitive to wavefront distortions. However, quantitative measurements of the effects of aberrations are not easy to obtain. We propose to use a liquid-crystal spatial light modulator as a programmable wavefront aberrator. This allows us to simulate experimentally a coherent detection system at  $\lambda = 632.8$  nm. Two frequency-shifted plane waves (backscattered signal and local oscillator) are generated. The programmable liquid-crystal wavefront aberrator is used to computer-control the phase of the backscattered signal, and the heterodyne efficiency is measured. We present experimental measurements of the field-of-view, the effect of defocus and the sensitivity to atmospheric perturbations. In all three cases, the experimental data are compared to the theoretical predictions. © 1999 Elsevier Science B.V. All rights reserved.

*Keywords:* Sensitivity; Heterodyne detection; Liquid-crystal modulator

---

## 1. Introduction

Heterodyne detection is a powerful technique to recover a small signal in noise, and is broadly used in many optronic-sensing devices [1–4]. It is usually based on the following optical configuration [5]: two frequency-shifted coherent beams are generated. The first one, the local oscillator, is kept in the system as a reference. The second one is used to illuminate a remote target, such as particles of dust in the atmosphere, which partially reflects it. A fraction of this backscattered signal is then collected. This wave carries useful information, such as the target Doppler frequency-shift in speed-sensing. However, in order to improve the signal-to-noise ratio when extracting this information, the backscattered signal must be demodulated by the local oscillator. This is possible because the two beams are, at least to a certain extent, partially coherent.

The local oscillator and the backscattered signal wavefronts are superimposed by a beam splitter, and then focused on a rapid detector. In the ideal case, the two wavefronts are plane, limited transversely by the same pupil and the beam splitter is aligned such that the waves are perfectly parallel. Hence, both focal spots have Airy distributions, and the interesting part of the electrical signal at the output of the detector is a signal beat, the so-called heterodyne signal, whose frequency is the difference between those of the backscattered signal and local oscillator. The heterodyne efficiency is expressed in the pupil as [5,6]:

$$\eta = \frac{\left| \int_{\text{PUPIL}} A_{\text{LO}}(r) A_{\text{BS}}(r) dr \right|^2}{\left( \int_{\text{PUPIL}} |A_{\text{BS}}(r)|^2 dr \right) \left( \int_{\text{PUPIL}} |A_{\text{LO}}(r)|^2 dr \right)}. \quad (1)$$

In the above formula,  $A_{\text{BS}}$  and  $A_{\text{LO}}$  are, respectively, the backscattered signal and local oscillator electric fields in the pupil, and the integrals are taken over all the surface

---

\* Corresponding author. E-mail: delautre@tco.thomson-csf.com

of the pupil. Note that the expression of the heterodyne efficiency  $\eta$  in the focal plane is exactly the same, but with the integration taken over the detector, provided the dimensions of the detector are sufficiently large compared to that of the Airy spots. Ideally,  $\eta$  should be equal to unity. This is the case if both Airy distribution spots have the same size, but not necessarily the same intensity. If the dimension of one of the two pupils changes, then the dimension of one spot changes as compared to the other, and  $\eta$  decreases consequently.

In practice, the backscattered signal wavefront is affected by the reflection on the target [7] and by the atmospheric perturbations [5] along the propagation path. The backscattered signal wavefront obtained on the pupil of the system then presents a speckled pattern, and its focal spot is broadened. Therefore, the portion of the backscattered signal spot interfering with the local oscillator spot decreases, and causes the heterodyne signal to fall down. Moreover, without even being distorted, the backscattered signal wavefront arriving on the pupil can possibly have a variable direction of propagation or tilt, which makes the backscattered signal and the local oscillator wavefronts misaligned and the focal spots not perfectly superimposed. In this case, the size of the interfering parts of the two spots decreases, and the heterodyne signal also falls down. Therefore, heterodyne detection is highly sensitive to every phenomenon which affects the form and the position of the backscattered signal spot on the detector, or equivalently to the aberrations of the backscattered wavefront. A simple calculation in the case of tilt can help understand this sensitivity. For a pupil  $D = 2$  cm wide, a focal length  $f = 25$  cm and a wavelength  $\lambda = 632.8$  nm, the width of the Airy distribution in the focal plane is  $d = 2.44\lambda f/D \approx 19 \mu\text{m}$ . If the two spots are separated by  $19 \mu\text{m}$ , they cancel almost exactly and  $\eta \approx 0$ . This happens when the backscattered signal is exactly tilted with an angle  $\theta \approx \tan \theta = d/f \approx 77 \mu\text{rad}$ , which is indeed very small. The sensitivity of heterodyne detection is theoretically well known, but although experimentally it has been qualitatively observed, precise quantitative measurements are very difficult to obtain. The reason for this is simple: in order to perform a systematic series of measurements, the experimenter has to be able to control precisely the phase of the backscattered signal wavefront. For instance, when measuring the influence of tilt on heterodyne efficiency, all possible tilt angles have to be generated and controlled.

An interesting solution has appeared in the last few years to achieve an arbitrary wavefront shape, which uses a programmable phase-modulating spatial light modulator (7SLM). Recently, Tataki and Ohzu [8,9] proposed and demonstrated the use of a pure-phase liquid-crystal SLM to modulate the transfer function of a fixed lens. This idea was extended in Ref. [10] to a twisted nematic liquid-crystal SLM, derived from a commercial liquid-crystal television. This is the wavefront aberrator we use in this work. Although this kind of SLM always shows coupled ampli-

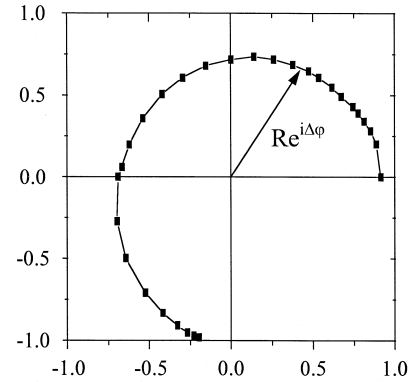


Fig. 1. From Ref. [10]: measured amplitude ( $R$ ) and phase ( $\Delta\varphi$ ) modulation characteristics for the twisted nematic liquid-crystal SLM used in the experiments for a 632.8 nm wavelength. Each point is obtained for a different voltage applied to an individual pixel of the SLM. As the SLM is driven by a frame grabber, voltages are represented as grey levels of the displayed image. The desired phase image is simply projected onto the modulation characteristic (see Ref. [10] for more details).

tude and phase modulation, and the phase modulation is limited to  $3\pi/2$  (see the phase-amplitude characteristics on Fig. 1), it was shown to provide accurate results for image translation and focus control. Translation and focus control are, respectively, achieved by displaying a Fresnel-prism-type or a Fresnel-lens-type phase function on the SLM. The reader is referred to Ref. [10] for more details. This programmable wavefront aberrator can be applied to generate any distorted phase screen, and especially to simulate atmospheric turbulence. The main idea of this article is to introduce such a twisted nematic liquid-crystal SLM in the pupil of a heterodyne detection system, in order to control the phase of the signal wavefront. Hence, the backscattered signal is artificially generated and smoothly controlled in the presented experiments. This allows us to investigate experimentally the sensitivity of heterodyne detection to wavefront aberrations.

The experimental set up is first introduced and described. The influence of misalignment, defocus and atmospheric turbulence on heterodyne efficiency are then studied experimentally and compared to theoretical predictions.

## 2. Experimental

The experimental set up is depicted on Fig. 2. The output of a He–Ne laser at  $\lambda = 632.8$  nm is injected in an acousto-optic modulator (AOM) driven by a 45-MHz acoustic signal. The 1st-order is deflected and frequency-shifted with respect to the 0th-order ( $\Delta\nu = 45$  MHz). These two beams then enter a Mach–Zehnder interferometer. In the first arm, the 0th-order is expanded and passed through a circular aperture, and serves as the local oscilla-

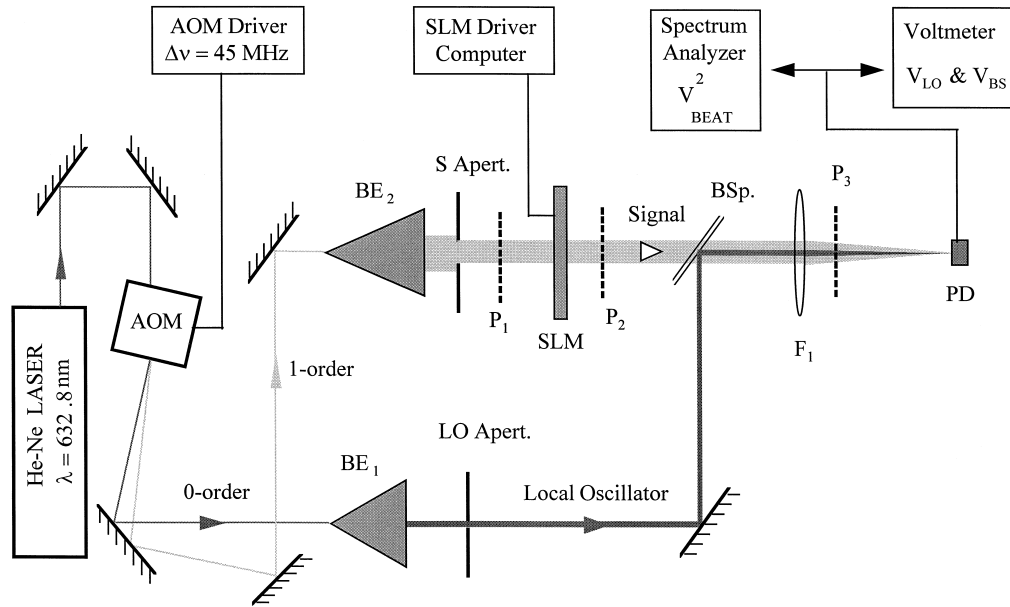


Fig. 2. Optical set up: AOM, acousto-optic modulator, 45 MHz; BE<sub>1</sub>, BE<sub>2</sub>, beam expanders; S Apert., signal aperture,  $\varnothing = 18$  mm; LO Apert., local oscillator aperture,  $\varnothing = 3$  mm; P<sub>1</sub>, P<sub>2</sub>, P<sub>3</sub>, polarizers; BSp, beam splitter; PD, photodetector, F<sub>1</sub>, focusing lens.

tor. In the second arm, the 1st-order is also expanded, passed through a circular aperture and controlled by the SLM wavefront aberrator. The 1st-order is used as the signal beam. Both beam-expander plus aperture groups are set up so that two plane waves are obtained with quasi-constant intensity. However, the local oscillator aperture is smaller than the signal one. The SLM aberrator system is composed of an input polarizer, a nematic-twisted liquid-crystal television, and an output polarizer. The relative orientations of the two polarizers are chosen so as to obtain the quasi-phase characteristics of Fig. 1. The SLM is driven by VGA signals, and provides  $640 \times 480$  independent pixels. Both local oscillator and signal beams are superimposed by a beam-splitter and then focused on a 1-mm photodiode using lens L<sub>1</sub>. The photodiode has a sufficiently large bandwidth to measure both the 45-MHz beat and the continuous signal. Since the local oscillator and signal apertures are different, the two spots are also different in size. However, both are sufficiently smaller than the detector, so that approximately all of the energy of both spots are collected. In these conditions, Eq. (1) can be replaced by:

$$\eta \approx \frac{\left| \int_{\text{DETECTOR}} A_{\text{LO}}(r) A_{\text{BS}}(r) dr \right|^2}{\left( \int_{\text{DETECTOR}} |A_{\text{BS}}(r)|^2 dr \right) \left( \int_{\text{DETECTOR}} |A_{\text{LO}}(r)|^2 dr \right)} \approx \frac{V_{\text{BEAT}}^2}{2V_{\text{BS}}V_{\text{LO}}} \quad (2)$$

This approximate formula allows for a quantitative evaluation of the heterodyne efficiency, since the numerator is proportional to the square of the root mean square beat voltage ( $V_{\text{BEAT}}^2$ ) given by the spectrum analyzer (peak value at 45 MHz), while the two terms of the denominator,  $V_{\text{BS}}$  and  $V_{\text{LO}}$ , are given by a voltmeter when masking one beam or the other. Therefore, in our set up, the heterodyne efficiency can be easily measured and plotted as a function of any kind of phase pattern generated by the SLM wavefront aberrator.

Fig. 3 shows the experimental field-of-view of our heterodyne detection system, i.e., the heterodyne efficiency

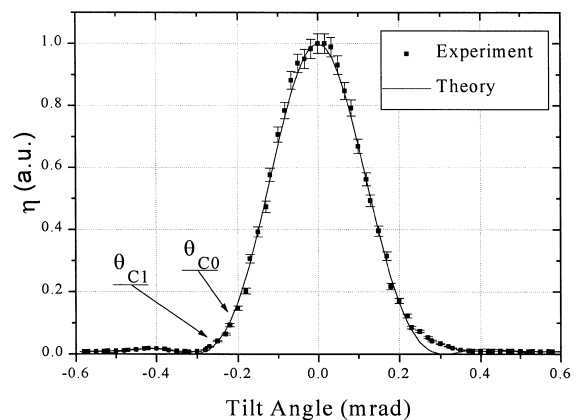


Fig. 3. Heterodyne efficiency ( $\eta$ ) as a function of the tilt angle  $\theta$  between local oscillator and signal wavefronts:  $\theta_{\text{CO}}$  cut-off angle for  $r_{\text{LO}} = 1.5$  mm;  $\theta_{\text{C1}}$  cut off angle for  $r_{\text{LO}} = 1.25$  mm.

as a function of the tilt angle  $\theta$  between local oscillator and signal wavefronts. This is a direct measurement of the sensitivity to misalignments. The tilt angle  $\theta$  is obtained by varying the slope of a Fresnel prism written onto the SLM [10]. It was shown [11], and using Ref. [12] that for two plane waves incident in the pupil with a relative angle  $\theta$ , and assuming constant amplitudes for  $A_{LO}$  and  $A_{BS}$  in the pupil,  $\eta$  is theoretically given by:

$$\eta = \left( \frac{r_{LO}}{r_{BS}} \right)^2 \left[ \frac{2J_1(k\theta r_{LO})}{k\theta r_{LO}} \right]^2. \quad (3)$$

In the above formula,  $r_{LO}$  and  $r_{BS}$  are the radii of the two circular apertures with  $r_{LO} < r_{BS}$  and  $k = 2\pi/\lambda$ . The theoretical curve of Fig. 3 is plotted for  $r_{LO} = 1.25$  mm, whereas the measured value is  $r_{LO} = 1.5$  mm. This difference can be explained by the fact that the intensity distributions of the two wavefronts are truncated Gaussian rather than truly uniform functions. Therefore, the widths of the two focal spots are broadened, which implies that the curve on Fig. 3 is larger than expected. However, on Fig. 3, the cut-off angle given by the antenna theorem [6,13], which is taken to be conventionally  $\theta_C = \lambda/(2r_{LO})$ , is estimated to be  $\theta_{C0} = 210 \mu\text{rad}$  with  $r_{LO} = 1.5$  mm, which is compatible with  $\theta_{C1} = 253 \mu\text{rad}$  obtained with  $r_{LO} = 1.25$  mm. From these results, it can be concluded that experiment and theory are in good agreement.

In order to determine the defocus sensitivity of the heterodyne efficiency, the same measurement technique can be used, but in this case, a Fresnel lens must be written onto the SLM [10], and its focal length varied progressively. In this way, the curvature of the signal beam is modified, whereas the local oscillator remains perfectly focused on the detector. The experimental results are shown in Fig. 4, where the heterodyne efficiency is plotted as a function of the defocus, expressed as a percentage of the focal length generated by the SLM normalized to

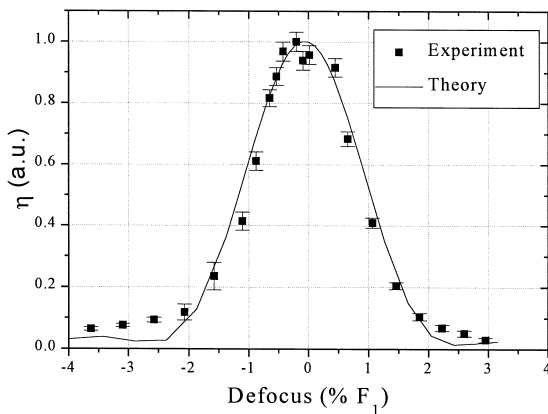


Fig. 4. Heterodyne efficiency ( $\eta$ ) as a function of the defocus (percentage of  $F_1 = 250$  mm).

the focal length of  $F_1$  ( $f = 250$  mm). The theoretical curve of Fig. 4 is obtained by numerical integration in the pupil plane, assuming plane waves with uniform illumination incident on the SLM and for the local oscillator, and taking into account the propagation between SLM and lens  $F_1$ . The local oscillator aperture dimension was taken to be  $r_{LO} = 1.5$  mm in this computation, i.e., the measured value, instead of 1.25 mm as in the case of the tilt angle. This can be explained by the fact that the heterodyne efficiency in the case of defocus is much less sensitive to the Gaussian non-uniformity of the wavefronts. Again, experiment and theory agree reasonably well, at least for small values of defocusing. For large defocus, the experimental heterodyne efficiency tends to a constant whereas theoretically, it should tend to zero. This can be explained by the fact that the SLM cannot display perfectly the high frequencies that appear for large defocus [10], so that there is always a background of undiffracted light coherent with the local oscillator.

### 3. Results and discussion

The tilt and defocus aberrations considered above are the most simple aberrations that can be conceived, and they serve well to qualify the robustness of heterodyne detection. However, for practical implementations, atmospheric propagation generates turbulent complex wavefronts. It is generally accepted that a good approximation to turbulence is provided by random correlated Kolmogorov phase screens [14]. In our method, prior to being written onto the SLM, these phase screens can be generated in the following way. First a two-dimensional array of size  $N \times N$  of uncorrelated Gaussian noise is generated with zero mean and variance  $\sigma^2 = (2\pi)^2/(\Delta b)^2$ , where  $\Delta b$  is the actual pixel dimension. A discrete Fourier transform is then applied to this array, and the resulting array is filtered to produce a desired power spectral density (PSD). According to previous works [14,15], the PSD of the phase  $\varphi$  induced by propagation in a medium with a strength of turbulence  $C_n^2$  constant along the path  $R$  is:

$$\Phi_\varphi(k) = 0.033(2\pi)^{-2/3} R \frac{C_n^2}{\lambda^2} (\Delta b N)^{11/3} k^{-11/3}, \quad (4)$$

where  $k = (i^2 + j^2)^{1/2}$  is the spatial frequency, with  $i$  and  $j$  the two indexes of the array numbered from 1 to  $N$ . Hence, the filter function is simply given by:

$$T_\varphi(k) = [\Phi_\varphi(k)]^{1/2}. \quad (5)$$

Fried [5] showed that the influence of the three factors  $R$ ,  $\lambda$  and  $C_n^2$  can be gathered in a simple parameter  $r_0$ , the Fried radius, which corresponds approximately to the mean

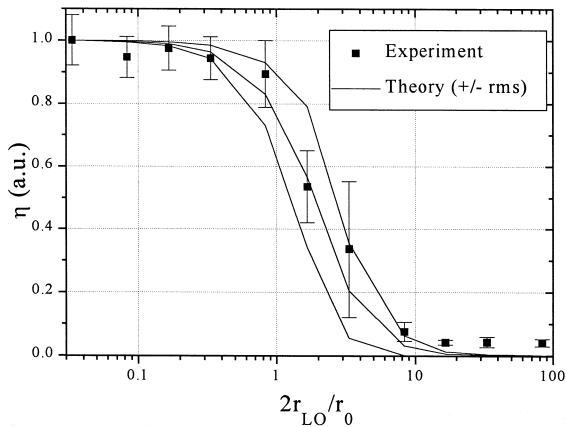


Fig. 5. Heterodyne efficiency ( $\eta$ ) as a function of the atmospheric turbulence represented by  $2r_{LO}/r_0$ ,  $r_0$ , Fried radius of the wavefront in the pupil plane;  $r_{LO}$ , radius of the local oscillator aperture.

diameter of the speckle cells in the pupil plane. Then,  $T_\varphi$  becomes:

$$T_\varphi(k) = \left[ 0.033(2\pi) \frac{6.88}{2.91} r_0^{-5/3} k \left( \frac{2\pi k}{N\Delta b} \right)^{-11/3} \right]^{1/2}. \quad (6)$$

Finally, a discrete inverse Fourier transform is applied to the filtered phase noise, and a Kolmogorov power law phase screen is obtained. Fig. 5 shows the experimental results. Note that for each value of  $(2r_{LO})/r_0$ , 16 phase patterns were generated and displayed on the SLM, so that a mean value and a variance could be approximately computed. The theoretical curve was generated by numerical integration in the pupil plane. For each value of  $(2r_{LO})/r_0$ , 100 phase patterns were generated, so that a mean value and a variance could be calculated with reasonable accuracy. Again, experiment and theory agree reasonably well, especially for large values of  $r_0$ . It can be seen that the heterodyne efficiency decreases when the diameter of the speckle cells ( $r_0$ ) is smaller than the diameter of the local oscillator aperture ( $r_{LO}$ ). For small values of  $r_0$ , the strength of the turbulence is such that the Kolmogorov phase screen varies very rapidly, and eventually tends to white noise. As the SLM cannot display perfectly these high frequencies [10], similarly to the case of defocus, there is always a background of undiffracted light which explains the non-zero experimental mean of the heterodyne efficiency for large values of  $(2r_{LO})/r_0$ .

We proposed a laboratory experiment which is able to simulate the behavior of a heterodyne detection system subjected to phase aberrations. Any kind of wavefront distortion can be introduced on the signal beam by using a liquid-crystal SLM. The SLM we have used is an inexpensive twisted nematic liquid-crystal television in VGA format ( $640 \times 480$  pixels), that can provide quasi-pure phase modulation in transmission. Using this system, we measured the sensitivity of heterodyne detection to tilt and defocus aberrations, and to atmospheric turbulence as represented by Kolmogorov phase screens. Experiment and theory agree well within the experimental errors.

### Acknowledgements

We are indebted to Jean-Louis Meyzonnette (Institut d'Optique Théorique et Appliquée, Orsay, France), Daniel Dolfi and Jean-Pierre Huignard (Thomson-CSF, Corporate Research Laboratories) for helpful discussions and suggestions.

### References

- [1] J.M. Vaughan, Coherent laser radar in Europe, Proc. IEEE 84 (1996) 205–226.
- [2] I. Melngailis et al., Laser radar component technology, Proc. IEEE 84 (1996) 227–267.
- [3] C. Karlsson, D. Letalick, M. Harris, G. Pearson, 9th Conference on Coherent Laser Radar, Linköping, Sweden (23–27 June 1997).
- [4] M. Kavaya, G. Emmitt, invited paper 3380-02, Proc. SPIE, Vol. 3380, Conference on Laser Radar Technology and Applications III, 12th Annual Symposium on Aerospace/Defense Sensing, Simulation and Controls, AeroSense, Orlando, FL (14 April 1998).
- [5] D. Fried, Proc. IEEE 55 (1967) 57.
- [6] R. Kingston, Detection of Optical and Infrared Radiation, Springer, Berlin, 1978.
- [7] W. Leeb, P. Winzer, K. Kudielka, Appl. Opt. 37 (1996) 3143.
- [8] Y. Tataki, H. Ohzu, Opt. Commun. 126 (1996) 123.
- [9] Y. Tataki, H. Ohzu, Appl. Opt. 35 (1996) 6896.
- [10] V. Laude, Opt. Commun. 153 (1998) 134–152.
- [11] S. Cohen, Appl. Opt. 14 (1975) 1953.
- [12] I. Gradshteyn, I. Ryzhik, Table of Integrals, Series and Products, Academic Press, New York, 1980.
- [13] A. Siegman, Proc. IEEE 54 (1966) 1350.
- [14] V. Tatarski, Wave Propagation in a Turbulent Media, Dover Publications, New York, 1961.
- [15] K. Gamble, A. Weeks, Proc. Soc. Phot-Opt. Instr. Eng. 2748 (1996) 220.